

Critical Behavior at the Nematic-to-Smectic-*A* Transition in a Nonpolar Liquid Crystal with Wide Nematic Range

Li Chen,⁽¹⁾ J. D. Brock,⁽²⁾ J. Huang,⁽¹⁾ and Satyendra Kumar⁽¹⁾

⁽¹⁾*Department of Physics and Liquid Crystal Institute, Kent State University, Kent, Ohio 44242*

⁽²⁾*School of Applied and Engineering Physics, Cornell University, Ithaca, New York 14853*

(Received 29 July 1991)

High-resolution x-ray scattering experiments to study the critical smectic-*A* fluctuations in the nematic phase have been performed on a mixture of two nonpolar, two-benzene-ring compounds. The ratio T_{NA}/T_{NI} ($=0.885$) for this mixture is much smaller than for previously studied similar materials. The smectic correlation lengths parallel and perpendicular to the smectic-layer normal are found to diverge anisotropically with characteristic exponents $\nu_{\parallel}=0.75 \pm 0.03$, $\nu_{\perp}=0.65 \pm 0.03$, and the susceptibility with $\gamma=1.24 \pm 0.05$.

PACS numbers: 64.70.Md, 61.10.-i, 61.30.Eb, 64.60.Fr

Since the pioneering work of McMillan [1], the nematic-to-smectic-*A* (*NA*) phase transition in thermotropic liquid crystals has been a subject of extensive theoretical and experimental studies. A convenient physical realization of the simplest freezing transition in nature, the *NA* transition is of fundamental scientific significance; however, the detailed nature of this apparently simple transition remains poorly understood. Theoretical attempts to understand the *NA* transition can be divided into two groups. The first group predicts isotropic divergence of the size of a correlated region of critical smectic-*A* fluctuations in the nematic phase. The values of the characteristic exponents ν_{\parallel} and ν_{\perp} , describing the divergence parallel and perpendicular to the smectic density wave, are predicted to be $\frac{1}{2}$ by the mean-field theories [1,2], and $\frac{2}{3}$ by de Gennes's analogy [3] to critical behavior of superfluid He. The second group includes theories based on the de Gennes model [4] and on the dislocation-mediated melting mechanism [5] which predict anisotropic divergence with $\nu_{\parallel}=2\nu_{\perp}$. On the experimental front, this transition has been studied by several experimental techniques including x-ray diffraction [6,7], quasielastic light scattering [8,9], and heat capacity [10,11]. Anisotropic critical fluctuations at this transition are a common empirical feature among all materials. However, the values of critical exponents are material dependent and the ratio of the correlation-length exponents determined by x-ray scattering lies between 1.2 and 1.5 [8–11]. The value of the susceptibility exponent γ lies between 1.10 and 1.53, and for several materials agrees with the predictions based on the He analogy within experimental uncertainties. Thus, some aspects of different models appear to be correct while none of them is right in its entirety. The situation is not hopeless. The hyperscaling relation, $2\nu_{\perp} + \nu_{\parallel} = 2 - \alpha$, where α is the heat-capacity exponent, holds for most of the materials, suggesting some underlying universal behavior.

This complex situation can, to some extent, be ascribed to a number of factors. Ideally, one would like to study systems in which only the smectic order parameter is im-

portant near the *NA* transition. Unfortunately, the coupling between the smectic and nematic order parameters is significant. In materials exhibiting a narrow nematic range, the nematic order parameter does not saturate before the *NA* transition occurs. As the smectic order parameter grows, it forces the nematic order parameter to grow with it. The coupling between the smectic and nematic order parameters can be significant enough to drive the *NA* transition first order. This coupling is frequently taken to scale with the ratio of transition temperatures T_{NA}/T_{NI} , which is a measure of the width of the nematic phase. Experimentally, critical exponents are known to change with this ratio. Mean-field arguments [1] predict the *NA* transition to be weakly first order for $T_{NA}/T_{NI} > 0.87$, while experimental results indicate that the crossover to second order occurs at ratios on the order of 0.94–0.99. A narrow nematic range is not the only possible complicating feature of the phase diagram. Other nearby critical, tricritical, triple, or multicritical points can also strongly affect the details of the *NA* transition. Such complicating features are normally observed for polar or complex molecules. A second, more subtle issue, predicted by de Gennes [3], has been demonstrated by Als-Nielsen *et al.* [12]. The smectic-*A* phase is an example of a system at its lower marginal dimension, where the long-range thermal fluctuations destroy true thermodynamic long-range order. These fluctuations can certainly affect the critical behavior of the system. Finally, many of the thermotropic liquid crystals previously studied were not chemically stable or could not be purified to a level sufficient for critical phenomena studies.

We report here results of a high-resolution x-ray diffraction study of the *NA* transition in the 4-4'-alkylazoxybenzene (*DnAOB*) homologous series. The sixth, seventh, and eighth members of this series exhibit [13] an isotropic-nematic-smectic-*A* phase sequence. The molecules of this series are simple and symmetric, as modeled by McMillan in his microscopic theory, with a simple phase diagram. The nematic range is widest for the sixth homolog. There are no complicating features

such as the presence of a smectic-*C* or a reentrant nematic phase which might influence the nature of the *NA* transition. Previous work on these materials and their mixtures has shown that there is no detectable anomaly in diamagnetic susceptibility [13], birefringence [14,15], and enthalpy change [13] at the *NA* transition of pure D6AOB. The *NA* phase transition becomes first order [14] for approximately 46% concentration of D8AOB in D7AOB. In high-sensitivity ac heat capacity studies of D7AOB and D6AOB mixtures, Huang *et al.* [16] find the heat capacity changes to become vanishingly small for mixtures with more than $\sim 70\%$ D6AOB. A light scattering study [8] of the twist elastic constant of D6AOB shows that the transition is continuous to within ~ 0.1 mK of T_c . These reports confirm that not only the nematic-to-smectic transition in the sixth homolog is second order, but also that it is well removed from the tricritical point. Additionally, $(T_{NI} - T_{NA})/T_{NI} = 0.118$ for D6AOB is nearly twice as large as for any other simple, two-benzene-ring nonpolar material studied to date. Thus, it is an ideal system in which to study the nematic-to-smectic-*A* transition. Unfortunately, the smectic-*A* phase in pure D6AOB is monotropic and is not stable against freezing for a long enough time to permit x-ray measurements. In order to ensure phase stability on time scales appropriate for these x-ray measurements, it is necessary to use a 90% D6AOB+10% D7AOB mixture. The nematic range and transition temperatures for this mixture are only slightly different from those of pure D6AOB, and $T_{NA}/T_{NI} = 0.885$ is very close to the theoretical value for a second-order transition.

We made measurements on three slightly different mixtures: 10.98, 10.36, and 10.57 wt.% D7AOB. The latter two mixtures were prepared after carefully purifying the compounds by high-performance liquid chromatography. Results for all samples were essentially the same within experimental errors, although T_{NA} for two samples was found to drift initially by 200 mK before stabilizing. For one sample, prepared under slightly different conditions, the initial drift was less than 50 mK. We attribute this slight drift in transition temperature to sample decomposition. Our results confirm that the critical exponents are not significantly affected by small decomposition, as previously reported [9].

The sample, 6 mm in diameter and ~ 1.4 mm thick, was sealed between two 8- μm -thick Mylar films. It was oriented in the nematic phase by a 2.5-kG magnetic field produced by a pair of SmCo₅ permanent magnets placed on either side of the sample. Significantly improved alignment was obtained when the stretching direction of two Mylar films was oriented parallel to the magnetic-field direction. The aligning field was applied perpendicular to the incident x-ray beam in the scattering plane. Temperature was controlled with a precision of ± 0.0003 K by a two-stage oven.

The x-ray diffraction experiment used a Cu $K\alpha_1$ emis-

sion line from an 18-kW Rigaku rotating-anode generator. The monochromator and analyzer were single-crystal Ge (1,1,1)-Bragg-reflection devices oriented in a nondispersive geometry. The incident beam intensity was monitored by scattering part of the monochromatic beam into a NaI(Tl) scintillation detector. Two *xy* slits with tantalum blades were used after the monochromator to mask off the Cu $K\alpha_2$ emission line and to define the vertical x-ray spot size. We chose to use only the brighter $K\alpha_1$ emission line to reduce the number of parameters in the data analysis. As a result, the longitudinal resolution can be modeled by a linear combination of three Lorentzians as opposed to the six Lorentzians that were previously needed [17] when both lines were used. Full widths of our resolution were $\Delta q_{\parallel} = 4 \times 10^{-4} \text{ \AA}^{-1}$ and $\Delta q_{\perp} = 1 \times 10^{-5} \text{ \AA}^{-1}$. The out-of-plane resolution, $\Delta q_z \cong 3.4 \times 10^{-2} \text{ \AA}^{-1}$, was measured with a perfect Si crystal in open detector configuration. As a check we used Soller slits to tighten the out-of-plane resolution to $5 \times 10^{-3} \text{ \AA}^{-1}$. The increased resolution did not change the measured line shape, as previously observed [17]. Therefore, we did not use the Soller slits in subsequent scans.

The longitudinal and in-plane transverse scans were performed over three decades of reduced temperature. In-plane sample mosaicity was measured at the temperature point closest to T_{NA} and also modeled by a Gaussian.

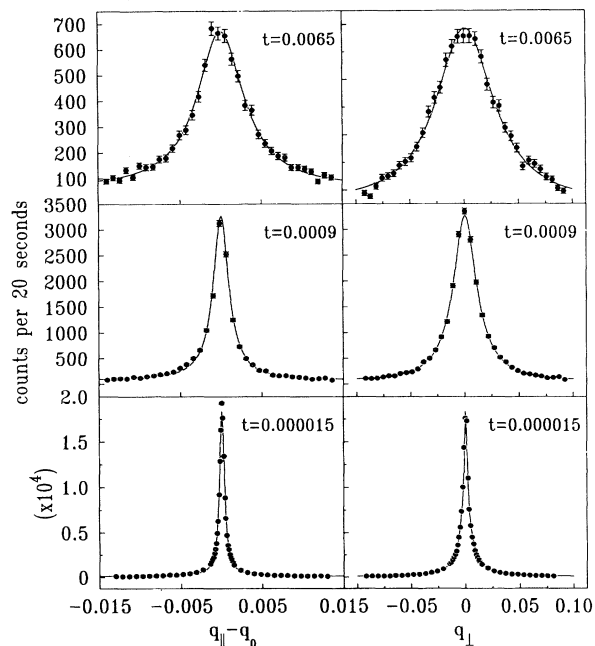


FIG. 1. Diffracted beam intensity plotted against $q_{\parallel} - q_0$ ($q_0 = 0.236 \text{ \AA}^{-1}$) for longitudinal scans and against q_{\perp} for transverse scans; at reduced temperatures $t = 1.5 \times 10^{-5}$, 9.0×10^{-4} , and 6.5×10^{-3} . Solid lines are fits by the smectic structure factor discussed in the text.

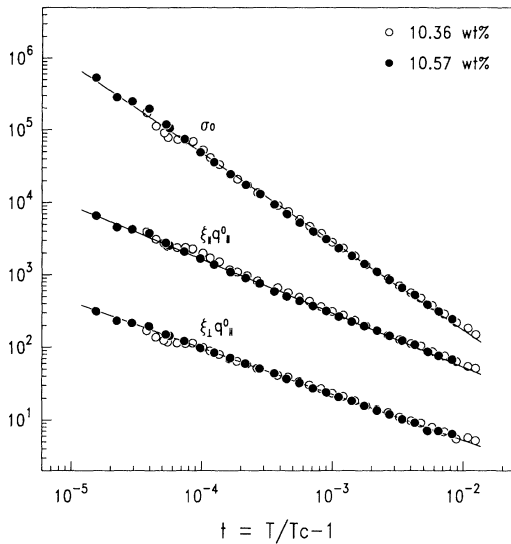


FIG. 2. Correlation lengths ξ_{\parallel} , ξ_{\perp} , and smectic susceptibility σ_0 vs reduced temperature. The solids lines are single power-law fits with exponents $\nu_{\parallel}=0.75 \pm 0.03$, $\nu_{\perp}=0.65 \pm 0.03$, and $\gamma=1.24 \pm 0.05$.

The instrumental resolution functions, corrections for energy broadening, and sample mosaicity were then convoluted with the smectic structure factor

$$S(\mathbf{q}) = \sigma_0 / [1 + \xi_{\parallel}^2 (q_{\parallel} - q_0)^2 + \xi_{\perp}^2 q_{\perp}^2 + C \xi_{\perp}^4 q_{\perp}^4]$$

and fitted to the data to obtain the correlation lengths ξ_{\parallel} , ξ_{\perp} , and the susceptibility σ_0 . Here, q_0 ($=0.236 \text{ \AA}^{-1}$) is the smectic wave vector which is nearly temperature independent for our sample. The fourth-order term is empirical and previously has been found necessary to describe the data [18].

Figure 1 shows representative longitudinal and transverse scans through the smectic density-wave peak at three different reduced temperatures. The solid lines are fits with the above line shape. The three quantities σ_0 , ξ_{\parallel} , and ξ_{\perp} obtained from such fits are shown in Fig. 2, for two different scans, as functions of reduced temperature. The solid lines are simple power-law fits of the type $\sigma_0(t) = \sigma_0^0 t^{-\gamma}$, $\xi_{\parallel}(t) = \xi_{\parallel}^0 t^{-\nu_{\parallel}}$, and $\xi_{\perp}(t) = \xi_{\perp}^0 t^{-\nu_{\perp}}$. Evidently, the temperature dependences of σ_0 , ξ_{\parallel} , and ξ_{\perp} are very well described by single power laws, ruling out any crossover behavior.

The best-fit values of the exponents are $\gamma=1.24 \pm 0.05$, $\nu_{\parallel}=0.75 \pm 0.03$, and $\nu_{\perp}=0.65 \pm 0.03$. The correlation lengths, clearly, diverge anisotropically. The transition temperature T_{NA} was also allowed to float in these fits. The values of T_{NA} obtained from fits were within 2 mK of the transition temperature obtained by monitoring the width of q_{\perp} (mosaic) scans. The values of the three exponents were slightly lower when the data were analyzed without mosaic correction, but well within the experimental errors of the above values. The mosaic width during

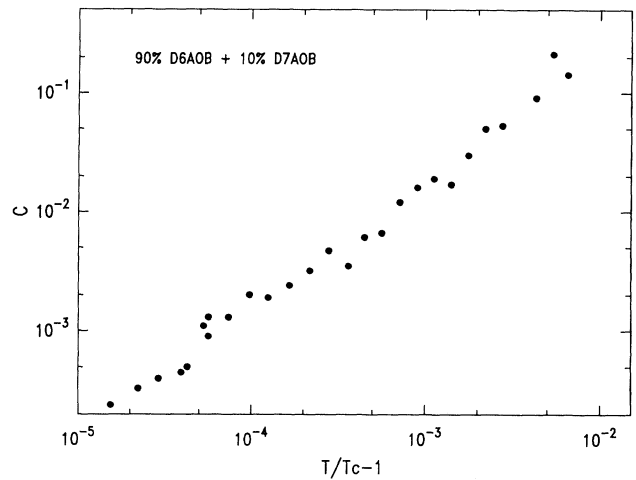


FIG. 3. Temperature dependence of the coefficient C of the fourth-order term in the smectic structure factor.

different scans varied between $5.3 \times 10^{-4} \text{ \AA}^{-1}$ (0.13°) and $4.6 \times 10^{-3} \text{ \AA}^{-1}$ (1.12°). For the scan with the most narrow (0.13°) mosaic, we obtained exponents, without a mosaic correction, that were essentially identical to those (given above) obtained for other scans with mosaic correction. The quoted errors in the exponents are from doubling of χ^2 and range shrinking. The best-fit value of the coefficient C changed with the reduced temperature, as shown in Fig. 3. C became relatively insignificant in the two decades of reduced temperature closest to T_{NA} as it remained below 6×10^{-3} . We found the bare correlation lengths, $\xi_{\perp}^0 \cong 1.0 \text{ \AA}$ and $\xi_{\parallel}^0 \cong 7.2 \text{ \AA}$, to be close to

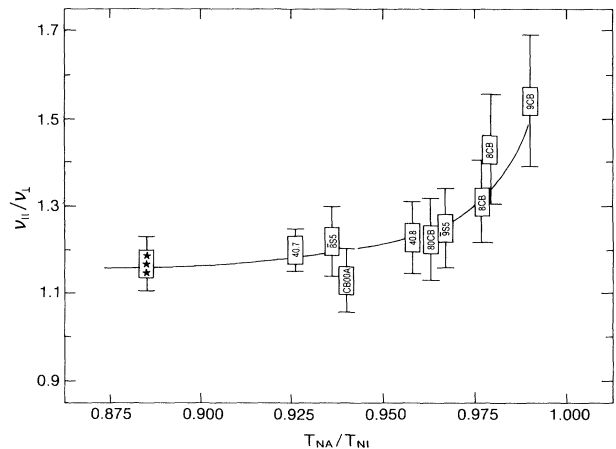


FIG. 4. Anisotropy, i.e., ratio of the critical exponents $\nu_{\parallel}/\nu_{\perp}$, vs T_{NA}/T_{NI} , for ten different materials taken from Refs. [8, 11, 17, 19]. The solid line is a guide to the eye and represents the trend. The point (***) at the lowest value of T_{NA}/T_{NI} is for the 90% D6AOB+10% D7AOB mixture. The two 8CB points are from x-ray diffraction experiments of Refs. [6] and [17].

those obtained for other materials [19].

The anisotropy, v_{\parallel}/v_{\perp} , calculated from the published values obtained by x-ray scattering for various materials is shown in Fig. 4. The point corresponding to the system we have studied is shown by three asterisks. With the help of our results a trend has, now, become evident. The anisotropy becomes gradually smaller with decreasing T_{NA}/T_{NI} and approaches an asymptotic value in the range 1.12–1.15. It should also be pointed out that for materials [8,11,17,20] (4O.7, 8S5, CBOOA, and 4O.8) with $T_{NA}/T_{NI} < 0.96$, a lower value of anisotropy is accompanied by a lower (than 1.53) susceptibility exponent γ . Even for highly polar materials [19] with wide nematic range, a comparatively small γ ($=1.22$) is obtained. The value of v_{\parallel} is in agreement with the bend-elastic-constant exponent, 0.75 ± 0.05 , recently measured with the quasielastic light scattering technique by Vithana *et al.* [8] on pure D6AOB. Additionally, the lack of crossover behavior in our results is also corroborated by their experiment.

In summary, we have measured the anisotropic growth of smectic fluctuations in the nematic phase as the system approaches the nematic-to-smectic-*A* phase transition in a nonpolar thermotropic liquid-crystalline material whose nematic range is almost twice that of any previously studied nonpolar material. Our results help provide a good overall picture of the *N*-*Sm-A* transition that should be valuable for theoretical understanding of this problem.

We acknowledge helpful discussions with Professor Dave Johnson, Professor Dave Litster, Professor Carl Garland, and Professor Daniel Finotello. This work was supported by the National Science Foundation under Grant No. DMR-88-19680.

[1] W. L. McMillan, Phys. Rev. A **4**, 1238 (1971).

[2] K. K. Kobayashi, J. Phys. Soc. Jpn. **29**, 101 (1970).

[3] P. G. de Gennes, Solid State Commun. **10**, 753 (1972);

C. Dasgupta and B. I. Halperin, Phys. Rev. Lett. **47**, 1556

(1981).

[4] T. C. Lubensky and A. J. McKane, J. Phys. (Paris), Lett. **43**, L-217 (1982).

[5] W. Helfrich, J. Phys. (Paris) **39**, 1199 (1978); D. R. Nelson and J. Toner, Phys. Rev. B **24**, 363 (1981).

[6] D. Davidov, C. R. Safinya, M. Kaplan, S. S. Dana, R. Schaezting, R. J. Birgeneau, and J. D. Litster, Phys. Rev. B **19**, 1657 (1979).

[7] K. K. Chan, P. S. Pershan, L. B. Sorensen, and F. Hardouin, Phys. Rev. A **34**, 1420 (1986).

[8] H. K. M. Vithana, V. Surendranath, M. Lewis, A. Baldwin, K. Eidner, R. Mahmood, and D. L. Johnson, Phys. Rev. A **41**, 2031 (1990), and references therein; G. Xu and D. L. Johnson (private communication).

[9] C. W. Garland, M. Meichle, B. M. Ocko, A. R. Kortan, C. R. Safinya, L. J. Yu, J. D. Litster, and R. J. Birgeneau, Phys. Rev. A **27**, 3234 (1983), and references therein.

[10] C. W. Garland, G. Nounesis, and K. Stine, Phys. Rev. A **39**, 4919 (1989), and references therein.

[11] R. Mahmood, H. Fellner, H. K. M. Vithana, J. Huang, and D. L. Johnson, Phys. Rev. A **41**, 6859 (1990), and references therein.

[12] J. Als-Nielsen, J. D. Litster, R. J. Birgeneau, M. Kaplan, C. R. Safinya, A. Lindegaard-Andersen, and S. Mathiesen, Phys. Rev. B **22**, 312 (1980).

[13] M. F. Achard, F. Hardouin, G. Sigaud, and H. Gasparoux, J. Chem. Phys. **65**, 1387 (1976).

[14] E. F. Gramsbergen and W. H. de Jeu, J. Chem. Soc. Faraday Trans. 2 **84**, 1015 (1988).

[15] W. H. de Jeu, Th. W. Lathouwers, and P. Bordewijk, Phys. Rev. Lett. **32**, 40 (1974).

[16] J. Huang *et al.* (private communication).

[17] B. M. Ocko, Ph.D. dissertation, Massachusetts Institute of Technology, 1984 (unpublished).

[18] J. Als-Nielsen, R. J. Birgeneau, M. Kaplan, J. D. Litster, and C. R. Safinya, Phys. Rev. Lett. **39**, 352 (1977).

[19] K. W. Evan-Lutterodt, J. W. Chung, B. M. Ocko, R. J. Birgeneau, C. Chiang, C. W. Garland, E. Chin, J. Goodby, and N. H. Tinh, Phys. Rev. A **36**, 1387 (1987).

[20] S. Sprunt, L. Solomon, and J. D. Litster, Phys. Rev. Lett. **53**, 1923 (1984).